HHS Public Access

Author manuscript

Cancer Res. Author manuscript; available in PMC 2020 January 01.

Published in final edited form as:

Cancer Res. 2019 July 01; 79(13): 3320–3331. doi:10.1158/0008-5472.CAN-18-2529.

Upregulation of scavenger receptor B1 is required for steroidogenic and non-steroidogenic cholesterol metabolism in prostate cancer

Jacob A. Gordon[1,2], **Jake W. Noble**[1], **Ankur Midha**[3], **Fatemeh Derakhshan**[4], **Gang Wang**[4], **Hans H. Adomat**[1], **Emma S. Tomlinson Guns**[1,2], **Yen-Yi Lin**[1], **Shancheng Ren**[5,†], **Collin C. Collins**[1], **Peter S. Nelson**[6], **Colm Morrissey**[7], **Kishor M. Wasan**[2,8], and **Michael E. Cox**[1,2,9,*]

[1]Vancouver Prostate Centre, Vancouver Coastal Health Research Institute, Vancouver, Canada

[2]Faculty of Pharmaceutical Sciences, University of British Columbia, Vancouver, Canada

[3]Institute of Immunology, Freie Universität Berlin, Berlin, Germany

[4]Department of Pathology, British Columbia Cancer Agency, Vancouver, Canada

[5]Department of Urology, Second Military Medical University, Shanghai, China

[6]Human Biology Division, Fred Hutchinson Cancer Research Center, Seattle WA, USA

[7]Department of Urology, University of Washington, Seattle, WA, USA

[8]College of Pharmacy and Nutrition, University of Saskatchewan, Saskatoon, Canada

[9]Department of Urologic Sciences, University of British Columbia, Canada

Abstract

Aberrant cholesterol metabolism is increasingly appreciated to be essential for prostate cancer (PCa) initiation and progression. Transcript expression of the high-density lipoprotein-cholesterol receptor scavenger receptor B1 (SR-B1) is elevated in primary PCa. Hypothesizing that SR-B1 expression may help facilitate malignant transformation, we document increased SR-B1 protein and transcript expression in PCa relative to normal prostate epithelium that persists in lethal castration-resistant prostate cancer (CRPC) metastasis. As intratumoral steroid synthesis from the precursor cholesterol can drive androgen receptor (AR) pathway activity in CRPC, we screened androgenic benign and cancer cell lines for sensitivity to SR-B1 antagonism. Benign cells were insensitive to SR-B1 antagonism, and cancer line sensitivity inversely correlated with expression levels of full-length and splice-variant AR. In androgen-responsive CRPC cell model C4-2, SR-B1 antagonism suppressed cholesterol uptake, de novo steroidogenesis, and AR activity. SR-B1 antagonism also suppressed growth and viability and induced endoplasmic reticulum stress and autophagy. The inability of exogenous steroids to reverse these effects indicates that AR pathway activation is insufficient to overcome cytotoxic stress caused by a decrease in the availability of

[†]For correspondences related to the Shanghai prostate cancer cohort. Department of Urology, Shanghai Changhai Hospital.

[*]**Corresponding Author Information:** Michael E. Cox, PhD, Associate Professor, Dept. of Urologic Sciences, University of British Columbia, Senior Scientist, The Vancouver Prostate Centre, mcox@prostatecentre.com - 1-604-875-4818, 2660 Oak Street, Vancouver, BC V6H 3Z6, CAN.

Conflict of Interest: The authors declare no potential conflicts of interest.

cholesterol. Furthermore, SR-B1 antagonism decreased cholesterol uptake, growth, and viability of the AR-null CRPC cell model PC-3, and the small molecule SR-BI antagonist Block Lipid Transport-1 decreased xenograft growth rate despite poor pharmacologic properties. Overall, our findings show that SR-B1 is upregulated in primary and castration-resistant disease and is essential for cholesterol uptake needed to drive both steroidogenic and non-steroidogenic biogenic pathways, thus implicating SR-B1 as a novel and potentially actionable target in CRPC.

INTRODUCTION

Cholesterol is essential for rapid cancer growth (1), and has been specifically linked to prostate cancer (PCa) progression to castration-resistant disease (CRPC) (2,3). Its levels are elevated in patient serum and bone metastasis post-androgen deprivation therapy (ADT), and hypercholesterolemia correlates with increased PCa-specific mortality (4–6). Additionally, association of elevated squalene monooxygenase (SQLE) expression with higher Gleason grade and disease-specific mortality indicates a role for *de novo* intratumoral cholesterol synthesis in lethal PCa (7). The increased appreciation that statin use is correlated with decreased PCa occurrence and improved disease prognosis (8–10), together with evidence linking statin use to improved PSA declines and overall survival in abiraterone-treated patients (11,12), highlight the benefit of reducing *de novo* cholesterol and androgen synthesis to achieve maximal suppression of androgen receptor (AR) pathway activation, and management of advanced PCa (13–16).

Cholesterol needs can also be met by elevating systemic uptake via the actions of low density lipoprotein receptor (LDLr) and scavenger receptors (SRs), particularly the Class B1 allele, SR-B1 (SCARB1) (17). LDLr transcript levels are lower in more aggressive tumors (7,18). Although elevated SCARB1 transcript levels have been suggested to correlate with decreased disease-free survival (18), analyses of the well-annotated Health Professional Follow-up, Physicians' Health Study, and Swedish Watchful Waiting cohorts demonstrated unchanged expression relative to tumor Grade or disease outcome (7). Whether SR-B1 expression persists in CRPC, and how it might promote mechanisms of malignant transformation, remain to be determined.

SR-B1 internalizes high density lipoprotein (HDL) cholesterol, and acetylated or oxidized LDL, and has allelic variants linked to increased risk of atherosclerosis and an impaired innate immune response (19). It is also critical for cholesterol uptake as a precursor for androgen synthesis in steroidogenic tissues (20). Experimentally, linkage of SR-B1 expression to PCa aggressiveness includes elevated expression in *de novo* androgenic CRPC derivatives of LNCaP (13,16), and increased tumor growth in TRAMP (21). SR-B1 also signals growth and survival of non-steroidogenic endothelial (22), and breast cancer cells (23), and association of elevated expression with aggressive characteristics and poor prognosis of breast, and clear cell renal carcinomas, indicates roles for SR-B1 in multiple malignancies (24–26).

Hypothesizing that SR-B1 expression may help facilitate malignant transformation by increasing levels of metabolically-available cholesterol, we demonstrate increased SR-B1 expression in the transition from normal prostatic tissue to cancerous tissue, and persistent

high expression in metastases. We go on to show sensitivity of androgenic PCa cell lines to SR-B1 antagonism, and how targeting SR-B1 suppresses cancer growth through induction of endoplasmic reticulum (ER) stress and autophagy via both steroid and non-steroid based mechanisms. These results implicate systemic cholesterol uptake mechanisms, particularly SR-B1, as potentially actionable targets for managing CRPC.

METHODS

Immunohistochemical (IHC) and mRNA expression analysis of clinical PCa samples:

IHC staining of the PCa Donor Rapid Autopsy Program at the University of Washington (UWRA, Seattle, WA) metastatic CRPC tissue microarray was performed using SR-B1 primary antibody: AB52629 (Abcam, Cambridge, United Kingdom) (27). Metastatic specimens were obtained from patients who died of metastatic CRPC, who signed written informed consent for a rapid autopsy performed within 6 h of death under the aegis of the PCa Donor Program at the University of Washington with Institutional Review Board approval. SR-B1 staining was scored by experienced independent pathologists (0 = no staining, 1 = low staining, 2 = moderate staining, 3 = high staining). Expression data for cholesterol metabolism gene transcripts was obtained from 27 patients with paired normal prostatic, and local cancerous, tissue from the Shanghai Changhai Hospital and Fudan University Shanghai Cancer Center (Shanghai Cohort, SC) (28) and from 83 CRPC patients from the UWRA; an expansion of the 63 CRPC patient data previously reported (27).

Cell culture:

The immortalized human prostate epithelial cell line, BPH-1, was generously provided by Dr. S. Hayward (NorthShore Research Institute, IL). PCa cell lines: C4-2, VCaP, 22Rv1, and PC3, were obtained from ATCC (Manassas, VA). BPH-1, 22Rv1 and PC3 were maintained in DMEM (Invitrogen, Burlington, ON, Canada) supplemented with 10% fetal bovine serum (FBS; Invitrogen). C4-2, was maintained in RPMI-1640 (Invitrogen) supplemented with 10% FBS. VCaP was maintained in low bicarbonate DMEM (ATCC) supplemented with 10% FBS. Unless otherwise noted, all other reagents were from VWR (Mississauga, ON) or Fisher Scientific (Ottawa, ON).

Block lipid transport-1 (BLT-1):

BLT-1 (ChemBridge, San Diego, CA), a selective inhibitor of cholesteryl ester transfer through SR-B1 (29), or dimethyl sulfoxide (DMSO, vehicle), was added to cells cultured in phenol red-free media supplemented with 5% charcoal-dextran stripped FBS (CSS, Invitrogen) at the indicated final concentrations. Unless otherwise specified, all assays were conducted 3 days post-treatment initiation.

RNA interference:

One day after transfection with either Stealth RNAi duplexes targeting SR-B1 (SRB1-KD: Oligo ID HSS101571: AUAAUCCGAACUUGUCCUUGAAGGG, Cat. No. 1299001) or Lo GC Negative Control duplexes (NC: Cat. No. 12935-110) (Invitrogen), cells were cultured in phenol red-free RPMI-1640 with 5% CSS for C4-2 cells, or DMEM with 10% FBS for PC3 cells (30). Unless otherwise specified, all assays were conducted 4 days post-transfection.

Androgen receptor (AR) activation reagents:

Metribolone (R1881, Perkin Elmer, Boston, MA), dehydroepiandrosterone (DHEA, Steraloids, Newport, RI), and progesterone (Sigma-Aldrich, St. Louis, MO) were added to culture medium simultaneously with BLT-1. DHEA was added to culture media 1 day post-SRB1-KD/NC transfection.

Immunoblotting:

Cellular protein levels were determined by immunoblot analysis as described in Supplementary Methods. Samples were normalized using primary antibodies targeting GAPDH (sc-32233) from Santa Cruz, and β-actin (A2228), or vinculin (V4505) from Sigma-Aldrich. Antibodies targeting the AR (sc-7305) was from Santa Cruz, SR-B1 (NB400-104) was from Novus Biologicals (Littleton, CO), and clusterin (CLU: 4214S and sc-6419) were from Cell Signaling (Danvers, MA) and Santa Cruz (Dallas, TX) in Figs 4 and 5, respectively. Antibodies targeting phospho-mTOR 923 (9234), mTOR (2983), BiP (3177), IRE1α (3294), p21 (2947), phospho-RB 807/811 (9308), phospho-RB 780 (9307), and LC3B (2775) were from Cell Signaling, and TP53 (OP03) was from EMD Millipore (Burlington, MA).

Cellular growth and viability:

Growth rates of BLT-1-treated or interfering RNA-transfected cells were determined by phase contrast image analysis using an Incucyte Zoom system (Essen Bioscience, Ann Arbor, MI) with confluency measured from sequential images used to determine cell growth kinetics using the system software. Propidium iodide (PI)- and annexin V-positive fractions were determined by automated image analysis at 72 h post-treatment initiation. The Live/Dead Cytotoxicity assay (Invitrogen) was performed following manufacturer instructions. Cell cycle analysis was performed using the previously described PI-based flow cytometry method (31).

HDL-cholesterol uptake:

HDL-derived cholesterol uptake was approximated using the fluorescent lipid, 1,1′-dioctadecyl-3,3,3′,3′-tetramethylindocarbocyanine perchlorate (DiI), from labelled HDL particles (DiI-HDL, Alfa Aesar, Haverhill, MA) as modified from established techniques described in Supplementary Methods (32).

Quantitative PCR:

Quantitative mRNA expression analysis was performed as described in Supplementary Methods using Qiagen (Toronto, Ontario, Canada) SYBR Green probes targeting SR-BI (QT00033488), HMGCR (QT00004081), PSA (QT00027713), and NKX3.1 (QT00202650) normalized to GAPDH (QT00079247).

Steroid analysis:

Cellular androgen levels were quantitatively assessed from ~100 mg cell pellets by LC-MS as previously described (15) and detailed in Supplementary Methods.

PSA secretion:

PSA secreted into media was quantified using an electrochemilluminescent immunoassay on a Cobas e 411 analyzer (Roche) and analyzed as previously described (15).

Fluorescence microscopy:

Formalin-fixed C4-2 cells were stained with wheat germ agglutinin (WGA) conjugated to Alexa Fluor 647 (WGA-647, Life Technologies) and 4′,6-diamidino-2-phenylindole (DAPI, Vector Laboratories, Burlington, ON) and imaged by confocal microscopy.

Senescence-activated β galactosidase (SA-βgal) Activity:

SA-βgal activity was detected in cells treated with 100 μM chloroquine for 2 h, then with 33 μM 5-dodecanoylaminofluorescein di-β-D-galactopyranoside (C_{12}FDG, Invitrogen) for 1 h prior to flow cytometry analysis as adapted from previously published methods (33).

Xenografts:

2×10^6 PC3 cells were inoculated subcutaneously on the hind flank of athymic nude mice (Crl:NU-Foxn1^{nu}; Harlan, Indianapolis, IN) under the auspices of UBC animal ethics protocol UBC ACC A16-0072. Tumor volumes (TV) were measured using calipers and the equation TV = length × width × height × 0.5326. Once tumors exceeded 100 mm^3, mice were randomized into vehicle (propylene glycol) or 25 mg/kg BLT-1 treatment (by oral gavage) cohorts administered daily for 4 weeks, or until tumor burden exceeded 10%, or weight loss exceeding 20%, in accordance with UBC committee on Animal Care standards.

Statistical analyses:

Statistical analyses were performed using GraphPad Prism (GraphPad, La Jolla, CA). Student's t-tests, chi-square tests, and ANOVA with Tukey's or Sidak's multiple comparisons test were used to determine differences between treatment groups. Means (± SEM) of the data sets were considered to be significantly different if $p < 0.05$.

RESULTS

SR-B1 is highly expressed in primary and metastatic PCa

We assessed SR-B1 expression in localized and metastatic PCa by comparing IHC staining of rapid autopsy specimens from the UWRA (27) to levels in clinical mRNA expression datasets. SR-B1 staining intensity in the UWRA samples of cancerous and patient-matched adjacent normal prostatic tissue, and of bone, lymph node, liver and lung metastasis rapid autopsy specimens, was scored as moderate to high in 24% of normal prostate samples (56 of 236 cores), in 71% of local PCa samples (167 of 236 cores), and in 57% of bone (118 of 207 cores), 77% of liver (42 of 54 cores), 84% of lymph node (56 of 67 cores), and 84% of lung (22 of 26 cores) metastasis samples (Fig. 1A,B). Further, statistical comparisons can be found in Table S1. Overall, these results indicated that SR-B1 expression is increased in both local and metastatic samples compared to normal prostatic tissue, with bone exhibiting lower expression when compared to other metastatic sites.

We used transcriptional profiling data of matched UWRA specimens to analyze expression of the SR-B1 transcript, SCARB1, and of related cholesterol metabolism regulators, LDLr and HMGCR, in metastatic PCa tissue (Fig. 1C). Consistent with our IHC analysis, we observed higher SCARB1 expression compared to LDLr and HMGCR, with the highest expression in liver metastasis, and the lowest expression in bone metastasis. Analysis of TCGA-aggregated transcript level data also demonstrated elevated SCARB1 and decreased LDLr levels in PCa and indistinguishable levels of HMGCR between benign and cancerous samples (Fig. S1). We assessed the consistency of these observations in a uniformly collected, independent PCa cohort: the SC radical prostatectomy series (28). Comparing transcript levels for the cholesterol influx proteins SCARB1 and LDLr, multiple mevalonate pathway enzymes, and the cholesterol efflux proteins ABCA1 and ABCG1, between treatment-naïve PCa and matched normal tissues (Fig. 1D), we determined that the PCa group exhibited increased expression of SCARB1, decreased expression of LDLr, and no difference in expression of the other factors. The consistent upregulation of SR-B1 expression in the assessed cancerous specimens provides validation that SR-B1 expression is upregulated in PCa, and the first demonstration that this elevated expression pattern persists in metastatic CPRC lesions. Further, the observed decreased LDLr expression, suggests a potential shift in the mechanism PCa cells use to obtain exogenous cholesterol necessary to meet the metabolic demands of a rapidly proliferating and metastatic disease (34).

SR-B1 antagonism halts AR-driven cell growth

Since cholesterol is the essential metabolic precursor for steroid synthesis and is essential for *de novo* steroidogenesis by Leydig cells, we assessed relative expression of SR-B1, and full-length and splice variant AR in a benign prostatic hyperplasia cell line, BPH-1, and three known AR-driven CRPC cell lines, C4-2, VCaP, and 22Rv1. SR-B1 expression was detected at generally equivalent levels in the four cell lines (Fig. 2A). Consistent with previous reports, full-length AR was robustly expressed by VCaP and C4-2 cells, and detected at much lower levels in BPH-1 and 22Rv1 cells, while AR splice variant levels were highest in 22Rv1 and VCaP cells.

We previously demonstrated that SR-B1 antagonism suppressed growth of LNCaP cells during CRPC progression (16). We next tested whether there was any differential sensitivity to SR-B1 antagonism on AR-driven growth of these cell lines. Cell viability was indistinguishable in BPH-1 cells treated with the small molecule SR-B1 inhibitor, BLT-1 (Fig. 2B,C). Treatment of the cancer lines with BLT-1 dose-dependently induced cell death of C4-2 (≥10-fold) and VCaP (~4-fold) as measured by increased PI uptake and annexin V staining, while 22Rv1 cell viability was indistinguishable (Fig. 2B,C). The insensitivity of the non-malignant BPH-1 line, and the relative sensitivity of PCa lines proportional to AR full length and splice variant levels, suggested an increased reliance on SR-B1 in C4-2 cells as compared to cells with higher full-length and/or splice variant AR levels.

As C4-2 appeared to be the most susceptible to SR-B1 inhibition, it was selected for further studies using the SR-B1-targeted RNA interference to silence expression (Fig. 2D). siSR-B1-C4-2 cells displayed complete growth arrest by 48 h post-transfection, while scr-C4-2 cells displayed progressive growth over the time course such that the growth rate of siSR-

B1-C4-2 cells was 84% less than that of scr-C4-2 cells (Fig. 2E). Similarly, BLT-1 treatment dose-dependently suppressed C4-2 cell growth by 17%, 81% and 95% at 1, 10 and 20 μM compared to the vehicle control, respectively, and replicated the growth arrest observed in siSR-BI-C4-2 cells at ≥ 10 μM. (Fig. 2F). These observations demonstrate SR-BI expression is critical for growth of C4-2 cells under androgen-deprived conditions.

To compare how varying doses of BLT-1 or siRNA suppression affected proliferation, or death rates, calcein AM ester hydrolysis, vital dye exclusion, and cellular DNA content were assessed. Despite the observed profound suppression of proliferation, siSR-B1-C4-2 cell viability was indistinguishable, albeit slightly lower, on average from that of scr-C4-2 cells (Fig. 2G). By cellular DNA content analysis, siSR-B1-C4-2 cells exhibited a 25% increase in G_0 /G_1 phase cells compared to scr-C4-2 cells and a 2-fold increase in sub-G_0 cells, suggesting that suppressed SR-BI expression did result in a modest cytotoxicity (Fig. 2H). At concentrations that replicated the growth arrest observed in siSR-BI-C4-2, BLT-1 treatment resulted in a dose-dependent decrease in viability: 20% at 10 μM, and 70% at 20 μM (Fig. 2G). Similarly, by DNA content analysis, 5 and 10 μM BLT-1 treatment increased the sub-G_0 phase population 5- and 6-fold, respectively, to approximately 20% of the population at 10 μM (Fig. 2H). These results indicate that SR-B1 antagonism induced both a G_0/G_1 growth arrest, and suggest a modest increase in cytotoxicity, particularly at high concentrations of BLT-1.

SR-B1 antagonism alters cholesterol metabolism of C4-2 cells

The ability of SR-B1 antagonism to reduce HDL-derived cholesterol uptake was assessed using RNA interference, and small molecule antagonism. Both siSR-B1 and BLT-1 significantly reduced DiI uptake in C4-2 cells (siSR-B1-C4-2 vs scr-C4-2: −39%, BLT-1 vs vehicle: −62%, Fig. 3A). SR-B1 transcript levels were reduced 65% in siSR-B1 cells relative to scr-C4-2 cells, while SR-B1 protein was nearly absent (Fig. 3B). We previously reported that HMGCR inhibition induced SR-B1 expression in LNCaP-derived castrated xenografts (15), so we assessed whether SR-B1 antagonism had the converse effect on HMGCR expression. Finding that HMGCR expression was more than doubled in siSR-B1-C4-2 cells relative to scr-C4-2 cells (Fig. 3B) suggests that under androgen-deprived conditions, there is a compensatory response for increased *de novo* cholesterol synthesis to SR-B1 knockdown in this hormone-responsive PCa model.

SR-B1 antagonism reduces cellular androgen accumulation and AR activity

SR-B1 is critical for providing HDL-cholesterol to steroidogenic tissues (35), and we previously demonstrated reduced PSA secretion from C4-2 cells following SR-B1 knockdown (16,20). We therefore examined how cellular androgen levels and AR activation were impacted by SR-B1 antagonism. C4-2 cells are steroidogenic under androgen-deprived conditions (30), however intracellular testosterone levels were decreased by nearly 60% in siSR-B1-C4-2 cells relative to scr-C4-2 (Fig. 3C) and dose-dependently by BLT-1 treatment (by approximately 50% and 65% at 5 and 10 μM relative to vehicle, respectively, Fig. 3D). Additionally, DHT levels were decreased by 80% in siSR-B1-C4-2 compared to scr-C4-2 cells, and 70% and 80% in 5 μM and 10 μM BLT-1-treated C4-2 cells, respectively, as compared to vehicle alone (Fig. 3C,D). These findings demonstrate the ability of SR-B1

antagonism to impede the accumulation of AR-activating androgens. Concurrently, transcript levels of the AR target genes: PSA and NKX3.1, were found to be suppressed by 86% and 43%, respectively, in siSR-B1-C4-2 compared to scr-C4-2 cells (Fig. 3B). Furthermore, PSA secretion was reduced five-fold in siSR-B1 cells, and dose-dependently up to five-fold in BLT-1-treated cells (Fig. 3E). The ability of both interfering RNA and small molecule approaches to reduce accumulation of intracellular androgens and AR-mediated signalling in androgen-deprived C4-2 cells emphasize the ability of SR-B1 antagonism to impede *de novo* steroidogenesis, and suggests that the observed decreased AR activation is likely due to reduced presence of AR activating androgens.

SR-B1 antagonism promotes growth arrest by inducing cell stress and autophagy

Although autophagy can be regulated by several independent mechanisms, mammalian target of rapamycin (mTOR) is generally considered to be the primary regulator (36). By western blot analysis, we observed that mTOR phosphorylation was noticeably decreased in siSR-B1-C4-2 cells, and dose-dependently decreased in response to BLT-1 treatment (Fig. 4A). Decreased mTOR phosphorylation was correlated with activation of autophagy pathways, through increased expression of precursor, and robust expression of mature, CLU in both siSR-B1-C4-2 cells and BLT-1 treated cells, and increased LC3I/II conversion observed siSR-B1-C4-2 cells (Fig. 4A). Induction of an autophagic phenotype was further supported by accumulation of perinuclear vacuoles visualized by fluorescent microscopy in siSR-B1-C4-2 cells (Fig. 4B). These observations suggest that decreased cholesterol import through SR-B1 antagonism promotes autophagic flux as a mechanism to promote survival in response to cell stress in a manner similar to that previously described (37).

Altered cholesterol metabolism can promote ER stress (38) that, in turn, promotes induction of autophagy (39). Consistent with this, both siSR-B1 knockdown, and BLT-1 treatment, of C4-2 cells strongly induced expression of the essential ER stress chaperone, BiP, and more modestly induced expression of the inducer of ER stress chaperones, IREα (Fig. 4A). Since ER stress and autophagy are appreciated to arrest growth (36), we interrogated the impact of SR-B1 antagonism on expression of cell cycle check point markers. siSR-B1-C4-2 cells exhibited hypophosphorylation of RB serine 780 and serine 807/811, and increased expression of p53 and p21 (Fig. 4A). We additionally observed that cell cycle and growth arrest in siSR-B1-C4-2 cells correlated with increased activity of SA-βgal (Fig. 4C). Though typically used as a senescence marker, upregulated SA-βgal activity is also known to be associated with autophagy (40). These results suggest that SR-B1 antagonism induces a strong autophagic phenotype that is at least in part through the activation of ER stress pathways that inhibit mTOR.

SR-B1 knockdown phenotype is not rescued by exogenous steroid

In order to determine whether the stress responses observed in androgen-deprived, and SR-B1-antagonized, C4-2 cells resulted from decreased *de novo* steroidogenesis and AR activation, cells were co-stimulated with testosterone precursors, progesterone and DHEA, and the testosterone mimetic, R1881, to bypass the requirement for uptake/conversion of cholesterol as an androgen source. None of these factors reversed the growth arrest effects seen with 10 μM BLT-1 treatment of androgen-deprived C4-2 cells (Fig. 5A). Further,

cytotoxicity, as measured through PI and annexin V staining, were not reversed by these factors (Fig. 5B,C). As DHEA was the most clinically relevant steroid assessed (41), further studies were performed combining DHEA treatment with NC or SR-B1-targeted RNA interference. In scr-C4-2 cells, DHEA stimulated a near ten-fold increase in AR activity as measured by PSA secretion (Fig. 5D). Consistent with observations in Fig. 3, basal AR activity in siSR-B1 C4-2 cells was ~20% that of unstimulated scr-C4-2 cells. While DHEA treatment did stimulate a near 10-fold increase in AR activity in siSR-B1 C4-2 cells, the repressed basal AR activity of siSR-B1 C4-2 cells meant the resulting DHEA-induced maximal activity remained indistinguishable from the basal activity of scr-C4-2 cells, some 75% less than that of the DHEA-stimulated scr-C4-2 cells.

AR activation is a driver of C4-2 proliferation (42), but since the threshold of signaling required to maintain optimal growth or survival is not precisely defined, we also assessed the impact of DHEA stimulation on cell cycle distribution of siSR-B1 C4-2 cells (Fig. 5E). The increased G_0/G_1 and sub-G_0 population of siSR-B1 C4-2 cells relative to scr-C4-2 cells were indistinguishable in the presence of DHEA. Lastly, DHEA stimulation did not affect the robust expression of CLU observed in siSR-B1-C4-2 cells relative to scr-C4-2 cells (Fig. 5F). We conclude that the arrested phenotype observed with SR-B1 antagonism correlates with reduced AR activation that cannot be restored solely by replenishing steroid levels.

SR-B1 antagonism induces robust cell death in androgen-independent PC3 cells

Since restoring intracellular androgen levels appeared to be insufficient to reverse the anti-proliferative effects of SR-B1 antagonism, we assessed how SR-B1 antagonism impacted proliferation and viability of the AR-null, androgen-independent PCa cell line, PC3 (43). SR-B1-targeted interfering RNA-silenced PC3 cells (siSR-B1-PC3) exhibited little SR-B1 protein expression, and suppressed HDL-cholesterol uptake by 81% relative to scr-transfected cells (scr-PC3), while HDL-cholesterol uptake was suppressed 38% in BLT-1-treated PC3 cells relative to vehicle-treated cells (Fig. 6A). These results were consistent with the impact of SR-B1 antagonism in C4-2 cells and presented the opportunity to assess the impact of SR-B1 antagonism on a non-steroidogenic, AR-independent PCa model.

Using a growth kinetics assay, scr-PC3 cells confluency increased from 15% to nearly 80%, while siSR-B1-PC3 cells showed essentially no increase in cell density over the time course, never surpassing 20% confluency (Fig. 6B). Similarly, vehicle-treated PC3 cells grew from an initial density of 8%, to approximately 50% confluency after 120 h, while BLT-1 treatment profoundly suppressed PC3 growth, with the lowest dose (1 μM) decreasing growth by 80% relative to vehicle, and the highest dose (20 μM) resulting in a nearly complete growth arrest (Fig. 6C). Using proliferative and death indexes to determine how SR-B1 antagonism impacts growth kinetics of PC3 cells, we observed siSR-B1 transfection to be strongly cytotoxic, with 80% of the population reporting as dead, compared to 15% of the scr-PC3 cell population (Fig. 6D). Using DNA content analysis, this response was linked to a profound induction of cell death in siSR-B1-PC3 cells as compared to scr-PC3 cells (Fig. 6E). In contrast, while dose-dependently sensitive, BLT-1-treated cells only displayed a significant induction of cell death at 20 μM (30%) when compared to the vehicle treated cells (Fig. 6D). BLT-1-treated cells, instead, underwent up to a 15% increase in G_0/G_1 arrest

relative to vehicle-treated cells, with little change in sub G_0 levels (Fig. 6E). Despite the cytotoxic differences between interfering RNA-transfected and small molecule-treated cells, the robust response of PC3 cells indicates the importance of non-AR mediated effects to SR-B1 antagonism bringing further credence to the impact of nutrient starvation and induction of cellular stresses.

BLT-1 administration reduces PC3 tumor growth

To date, there are no reports assessing BLT-1 as a pharmacologic agent in mice. In order to determine if potentially efficacious levels of circulating BLT-1 could be achieved, serum samples were obtained from mice dosed by oral gavage to develop a pharmacokinetic profile. Mice dosed with 25 mg/kg BLT-1 had a Cmax of 552.5 ng/mL (2.28 μM) at 0.5 h post-dose, the first measured time point (Fig. S2A). The elimination half-life was 10.4 h, with a final concentration, measured 24 h post dose, of 0.783 ng/mL (0.189 μM) for a calculated $AUC_{0-\infty}$ of 3971.2 ng*hr/mL. Furthermore, BLT-1 was rapidly metabolized by liver microsomes having a half-life of 8 min (Fig. S2B). Mice dosed with 50 mg/kg BLT-1 were observed to suffer evidence of liver and kidney toxicity (Table S2).

Since PC3 cell growth was more sensitive to BLT-1 than C4-2 cells, with a nearly complete cessation of growth observed with 1 μM BLT-1, we concluded that 25 mg/kg would be a sustainable daily dose that could achieve the *in vitro* therapeutic dose for PC3 cells to assess whether it might impact xenograft growth. Over the treatment course, neither 25 mg/kg BLT-1, nor vehicle dosing impacted body weight or behaviour (Fig. S3). Although all mice displayed progressive tumor growth over the experiment course, the 5.4-fold increase in tumor growth in the BLT-1 cohort was significantly less than the 7.5-fold increase in the vehicle-treated cohort (Fig. 6F, Table S3). Using a linear regression model as previously described (15), tumor growth rate of the BLT-1 cohort (110.3 ± 9.28 mm^3/week) was ~30% less than the vehicle cohort (156.6 ± 10.74 mm^3/week). These results indicate that, despite a narrow therapeutic window, BLT-1 is capable of slowing PC3 tumor growth as a single agent.

DISCUSSION

Increased SR-B1 expression has been suggested to be related to aggressive characteristics in several cancer types (24,25), however, its role in PCa remains enigmatic. Here, we validate increased SR-B1 expression in localized PCa by comparison to adjacent normal prostatic tissue, and present the first evidence for persistent elevated expression in metastatic lesions where, anecdotally, specimens displaying high SR-B1 expression exhibited staining predominantly along the plasma membrane of carcinoma cells adjacent to stroma. While lower SR-B1 expression in bone metastasis could be attributed to effects of decalcification on antigenicity (44), decreased SCARB1 mRNA levels in matched specimens are consistent with these IHC observations. These corroborative findings, combined with the increasing appreciation of a role for cholesterol accumulation in disease aggressiveness, implicate SR-B1 as a factor in PCa progression.

SR-B1 antagonism using interfering RNA and small molecule approaches lead to robust reduction of PCa cell growth *in vitro*, while small molecule treatment resulted in a moderate

reduction in xenograft growth. Here, we describe how SR-B1 inhibition reduces androgen accumulation and AR activation in steroidogenic PCa cells, however, the differential responses of PCa models underscores the heterogeneous nature of the disease. The cell lines used represent distinct recurrent CRPC phenotypes. C4-2 maintain AR activation and signaling through *de novo* steroidogenesis (45,46). Similarly, VCaP harbor steroidogenic potential, but also express higher levels of full-length and splice variant AR isoforms (47), while 22Rv1 are predominantly AR splice variant-driven (48), and PC3 are fully AR-independent (49). In CRPC, AR-driven lipogenesis is associated with poor prognosis and linked to AR splice variant expression (50). The decreased sensitivity of VCaP, and insensitivity of 22Rv1, to BLT-1 treatment, are consistent with the possibility that AR splice variant expression could be sufficient to bypass the need for de novo cholesterol synthesis, or to drive lipogenic pathways under ARPI conditions (50).

Management of metastatic CRPC with second-line ARPIs (51,52), and indication that HMGCR inhibition can restore castration sensitivity of CRPC models (50,53), implicate a role for *de novo* steroidogenesis in ARPI resistance. If inhibition of HDL-derived cholesterol uptake through SR-B1 also impacts androgen accumulation by impeding *de novo* steroidogenesis, SR-B1 antagonism offers the potential to overcome several proposed mechanisms of ARPI resistance, including CYP17A1 amplification, and intratumoral accumulation of higher order steroids, and AR mutations that allow for responsiveness to steroid precursors (46,54,55). However, our previous observation that statin treatment increased SR-B1 expression in LNCaP xenografts (15), and here that SR-B1 antagonism increased HMGCR expression in C4-2 cells, suggest that these mutually compensatory mechanisms should be considered to take best advantage of targeting cholesterol availability in CRPC. Furthermore, these results suggest that effectiveness of targeting SR-B1 to suppress intratumoral steroidogenesis might be limited to full-length AR expressing CPRCs.

Cancer cells enduring nutritional, or other external, stresses employ survival mechanisms, including autophagy, in which cells degrade and recycle cellular constituents to meet metabolic demands (40). Autophagic responses to PCa treatments are common, and include responses to ADT and ARPIs, taxanes and kinase inhibitors (36). mTOR is an essential regulator of autophagy (36), and here is linked to induction of perinuclear vacuoles, LC3 lipidation and CLU expression. Inhibiting *de novo* lipogenesis in CPRC models reduces growth, and suppresses mTOR activity, and HMGCR and AR expression (50,53). Additionally, perturbing lipid and cholesterol homeostasis induce activation of ER stress and the unfolded protein response (UPR) (56,57). During the UPR, IRE1α activation leads to activation of key genes responsible for preventing hypocholesterolemia, and may therefore drive compensatory alterations in HMGCR expression (58). Such adaptations may underlie the enhanced efficacy of combining ARPIs with biguanides to disrupt mTOR nutrient sensor pathways, and statins to suppress *de novo* cholesterol synthesis (59).

The ability of AR pathway activation to negatively regulate autophagic activity under sub-optimal environmental conditions, such as culturing in charcoal stripped serum, was initially considered (55), however, R1881, DHEA and progesterone were unable to reverse the effects of SR-B1 antagonism. Although DHEA is a weak AR activator, it serves as precursor to more potent AR activating androgens (56), and potently induced AR activity in these

studies. The inability of DHEA to return AR activity to non-SR-B1-antagonized levels indicates that reduced *de novo* androgen synthesis, due to reduction of precursor, is but part of other extra-steroidal effects of SR-B1 antagonism that result in induction of an ER stress response program. While SR-B1 knockdown induced an autophagic response in C4-2 cells, it resulted in a strong cytotoxicity in PC3 cells, even though PC3 cells are capable of becoming autophagic following treatment with 26S proteosome or mTOR inhibitors (37,49). The lack of any AR axis-mediated signaling may impact their ability to initiate anti-proliferative, but pro-survival, stress responses resulting in a nutrient-depleted induction of cellular death. Therefore, the loss of AR functionality in an increasing fraction of patients failing second line ARPIs (50), may help identify patients particularly sensitive to SR-BI targeting.

BLT-1 is an established SR-B1-selective small molecule inhibitor, found to enhance HDL binding to SR-B1 but prevent intracellular transfer of cholesterol or cholesteryl ester (32). While not ideal for further development due to high hydrophobicity (60), rapid metabolism, and toxicity at high concentrations, sufficiently efficacious circulating BLT-1 levels were achieved to slow PC3 xenograft growth. In light of the hepato- and nephrotoxicity of the 50 mg/kg BLT-1 dosing, it is possible that xenograft growth was impacted, at least in part, because of subclinically impaired general health of the 25 mg/kg-treated mice. Despite this caveat, the combined results of these proof-of-principle findings indicate that SR-B1 antagonism can impact CRPC growth. These findings identify SR-B1 as an important contributing factor in the sustained proliferation of malignant prostatic disease, and highlight the potential for development of a novel SR-B1 inhibitor designed with intention for *in vivo* use. The ability of SR-B1 antagonism to arrest growth independent of AR activity, while also reducing AR activity in steroid-responsive PCa, provides a promising therapeutic prospect across the CRPC spectrum.

Supplementary Material

Refer to Web version on PubMed Central for supplementary material.

ACKNOWLEDGEMENTS

We thank Mary Bowden, Lisha Brown and Mei Yieng Chin for animal husbandry support, and Jonathan Frew for confocal microscopy assistance. We thank the patients and their families, Celestia Higano, Evan Yu, Heather Cheng, Bruce Montgomery, Elahe Mostaghel, Mike Schweizer, Andrew Hsieh, Dan Lin, Funda Vakar-Lopez, Lawrence True, and the rapid autopsy teams for their contributions to the UWRA program.

GRANT SUPPORT

This work is supported by the Prostate Cancer Foundation BC and Prostate Cancer Canada (2012-917). The UWRA tissue acquisition was supported by the Department of Defense Prostate Cancer Biorepository Network (PCBN) (W81XWH-14-2-0183), the Pacific Northwest Prostate Cancer SPORE (P50CA97186), the PO1 NIH grant (PO1 CA163227), and the Institute for Prostate Cancer Research (IPCR).

REFERENCES

1. Swyer GIM. The cholesterol content of normal and enlarged prostates. Cancer Res 1942;2:372–5.
2. Jeon JC, Park J, Park S, Moon KH, Cheon SH. Hypercholesterolemia Is Associated with a Shorter Time to Castration-Resistant Prostate Cancer in Patients Who Have Undergone Androgen Deprivation Therapy. World J Men Health 2016;34:28–33.

3. Pelton K, Freeman MR, Solomon KR. Cholesterol and prostate cancer. Curr Opin Pharmacol 2012;12:751–9. [PubMed: 22824430]
4. Yannucci J, Manola J, Garnick MB, Bhat G, Bubley GJ. The effect of androgen deprivation therapy on fasting serum lipid and glucose parameters. J Urol 2006;176:520–5. [PubMed: 16813881]
5. Batty GD, Kivimaki M, Clarke R, Smith GD, Shipley MJ. Modifiable risk factors for prostate cancer mortality in London: forty years of follow-up in the Whitehall study. Cancer Causes Control 2011;22:311–8. [PubMed: 21116843]
6. Thysell E, et al. Metabolomic characterization of human prostate cancer bone metastases reveals increased levels of cholesterol. Plos One 2010;5:e14175. [PubMed: 21151972]
7. Stopsack KH, et al. Cholesterol uptake and regulation in high-grade and lethal prostate cancers. Carcinogenesis 2017;38:806–11. [PubMed: 28595267]
8. Yu O, et al. Use of statins and the risk of death in patients with prostate cancer. J Clin Oncol 2014;32:5–11. [PubMed: 24190110]
9. Larsen SB, et al. Postdiagnosis Statin Use and Mortality in Danish Patients With Prostate Cancer. J Clin Oncol 2017;35:3290–7. [PubMed: 28806117]
10. Alfaqih MA, Allott EH, Hamilton RJ, Freeman MR, Freedland SJ. The current evidence on statin use and prostate cancer prevention: are we there yet? Nat Rev Urol 2017;14:107–19. [PubMed: 27779230]
11. Di Lorenzo G, et al. Statin Use and Survival in Patients with Metastatic Castration-resistant Prostate Cancer Treated with Abiraterone Acetate. Eur Urol Focus 2017;4:874–9. [PubMed: 28753882]
12. Gordon JA, et al. Statin use and survival in patients with metastatic castrationresistant prostate cancer treated with abiraterone or enzalutamide after docetaxel failure: the international retrospective observational STABEN study. Oncotarget 2018;9:19861–73. [PubMed: 29731989]
13. Leon CG, et al. Alterations in Cholesterol Regulation Contribute to the Production of Intratumoral Androgens During Progression to Castration-Resistant Prostate Cancer in a Mouse Xenograft Model. Prostate 2010;70:390–400. [PubMed: 19866465]
14. Kim JH, Cox ME, Wasan KM. Effect of simvastatin on castration-resistant prostate cancer cells. Lipids Health Dis 2014;13:56. [PubMed: 24666612]
15. Gordon JA, et al. Oral simvastatin administration delays castration-resistant progression and reduces intratumoral steroidogenesis of LNCaP prostate cancer xenografts. Prostate Cancer Prostatic Dis 2016;19:21–7. [PubMed: 26238234]
16. Twiddy AL, Cox ME, Wasan KM. Knockdown of scavenger receptor Class B Type I reduces prostate specific antigen secretion and viability of prostate cancer cells. Prostate 2012;72:955–65. [PubMed: 22025344]
17. PrabhuDas MR, et al. A Consensus Definitive Classification of Scavenger Receptors and Their Roles in Health and Disease. J Immunol 2017;198:3775–89. [PubMed: 28483986]
18. Schörghofer D, et al. The HDL receptor SR-BI is associated with human prostate cancer progression and plays a possible role in establishing androgen independence. Reprod Biol Endocrinol 2015;13:88. [PubMed: 26251134]
19. Krieger M Scavenger receptor class B type I is a multiligand HDL receptor that influences diverse physiologic systems. J Clin Invest 2001;108:793–7. [PubMed: 11560945]
20. Azhar S, Reaven E. Scavenger receptor class BI and selective cholesteryl ester uptake: partners in the regulation steroidogenesis. Mol Cell Endocrinol 2002;195:1–26. [PubMed: 12354669]
21. Llaverias G, et al. A Western-type diet accelerates tumor progression in an autochthonous mouse model of prostate cancer. Am J Pathol 2010;177:3180–91. [PubMed: 21088217]
22. Mineo C, Yuhanna IS, Quon MJ, Shaul PW. High density lipoprotein-induced endothelial nitric-oxide synthase activation is mediated by Akt and MAP kinases. J Biol Chem 2003;278:9142–9. [PubMed: 12511559]
23. Danilo C, Gutierrez-Pajares JL, Mainieri MA, Mercier I, Lisanti MP, Frank PG. Scavenger receptor class B type I regulates cellular cholesterol metabolism and cell signaling associated with breast cancer development. Breast Cancer Res 2013;15:R87. [PubMed: 24060386]

24. Li J, Wang J, Li M, Yin L, Li XA, Zhang TG. Up-regulated expression of scavenger receptor class B type 1 (SR-B1) is associated with malignant behaviors and poor prognosis of breast cancer. Pathol Res Pract 2016;212:555–9. [PubMed: 27067809]
25. Yuan B, et al. High scavenger receptor class B type I expression is related to tumor aggressiveness and poor prognosis in breast cancer. Tumour Biol 2016;37:3581–8. [PubMed: 26456958]
26. Xu G, et al. Diagnostic and prognostic value of scavenger receptor class B type 1 in clear cell renal cell carcinoma. Tumour Biol 2017;39:1010428317699110. [PubMed: 28466781]
27. Kumar A, et al. Substantial interindividual and limited intraindividual genomic diversity among tumors from men with metastatic prostate cancer. Nat Med 2016;22:369–78. [PubMed: 26928463]
28. Ren S, et al. Whole-genome and Transcriptome Sequencing of Prostate Cancer Identify New Genetic Alterations Driving Disease Progression. Eur Urol 2018;73:322–39.
29. Nieland TJ, Penman M, Dori L, Krieger M, Kirchhausen T. Discovery of chemical inhibitors of the selective transfer of lipids mediated by the HDL receptor SR-BI. Proc Natl Acad Sci USA 2002;99:15422–7. [PubMed: 12438696]
30. Locke JA, et al. Androgen levels increase by intratumoral de novo steroidogenesis during progression of castration-resistant prostate cancer. Cancer Res 2008;68:6407–15. [PubMed: 18676866]
31. Nunez R DNA measurement and cell cycle analysis by flow cytometry. Curr Issues Mol Biol 2001;3:67–70. [PubMed: 11488413]
32. Nieland TJ, Penman M, Dori L, Krieger M, Kirchhausen T. Discovery of chemical inhibitors of the selective transfer of lipids mediated by the HDL receptor SR-BI. Proc Natl Acad Sci USA 2002;99:15422–7. [PubMed: 12438696]
33. Debacq-Chainiaux F, Erusalimsky JD, Campisi J, Toussaint O. Protocols to detect senescence-associated beta-galactosidase (SA-betagal) activity, a biomarker of senescent cells in culture and in vivo. Nat Protoc 2009;4:1798–806. [PubMed: 20010931]
34. Luo X, et al. Emerging roles of lipid metabolism in cancer metastasis. Mol Cancer 2017;16:76. [PubMed: 28399876]
35. Wyatt AW, Gleave ME. Targeting the adaptive molecular landscape of castration-resistant prostate cancer. EMBO Mol Med 2015;7:878–94. [PubMed: 25896606]
36. Farrow JM, Yang JC, Evans CP. Autophagy as a modulator and target in prostate cancer. Nat Rev Urol 2014;11:508–16. [PubMed: 25134829]
37. Zhang F, et al. Clusterin facilitates stress-induced lipidation of LC3 and autophagosome biogenesis to enhance cancer cell survival. Nat Commun 2014;5:5775. [PubMed: 25503391]
38. Rohrl C, et al. Endoplasmic reticulum stress impairs cholesterol efflux and synthesis in hepatic cells. J Lipid Res 2014;55:94–103. [PubMed: 24179149]
39. Wang M, Wey S, Zhang Y, Ye R, Lee AS. Role of the unfolded protein response regulator GRP78/BiP in development, cancer, and neurological disorders. Antioxid Redox Signal 2009;11:2307–16. [PubMed: 19309259]
40. Gerland LM, Peyrol S, Lallemand C, Branche R, Magaud JP, Ffrench M. Association of increased autophagic inclusions labeled for beta-galactosidase with fibroblastic aging. Exp Gerontol 2003;38:887–95. [PubMed: 12915210]
41. Wang X, et al. Association of SLCO2B1 Genotypes With Time to Progression and Overall Survival in Patients Receiving Androgen-Deprivation Therapy for Prostate Cancer. J Clin Oncol 2016;34:352–9. [PubMed: 26668348]
42. Snoek R, et al. In vivo knockdown of the androgen receptor results in growth inhibition and regression of well-established, castration-resistant prostate tumors. Clin Cancer Res 2009;15:39–47. [PubMed: 19118031]
43. Chlenski A, Nakashiro K, Ketels KV, Korovaitseva GI, Oyasu R. Androgen receptor expression in androgen-independent prostate cancer cell lines. Prostate 2001;47:66–75. [PubMed: 11304731]
44. Bussolati G, Leonardo E. Technical pitfalls potentially affecting diagnoses in immunohistochemistry. J Clin Pathol 2008;61:1184–92. [PubMed: 18326011]
45. Horoszewicz JS, et al. LNCaP model of human prostatic carcinoma. Cancer Res 1983;43:1809–18. [PubMed: 6831420]

46. Cai C, et al. Intratumoral de novo steroid synthesis activates androgen receptor in castration-resistant prostate cancer and is upregulated by treatment with CYP17A1 inhibitors. Cancer Res 2011;71:6503–13. [PubMed: 21868758]
47. Knuuttila M, et al. Castration induces up-regulation of intratumoral androgen biosynthesis and androgen receptor expression in an orthotopic VCaP human prostate cancer xenograft model. Am J Pathol 2014;184:2163–73. [PubMed: 24949550]
48. Tepper CG, et al. Characterization of a novel androgen receptor mutation in a relapsed CWR22 prostate cancer xenograft and cell line. Cancer Res 2002;62:6606–14. [PubMed: 12438256]
49. van Bokhoven A, et al. Molecular characterization of human prostate carcinoma cell lines. Prostate 2003;57:205–25. [PubMed: 14518029]
50. Han W, et al. Reactivation of androgen receptor-regulated lipid biosynthesis drives the progression of castration-resistant prostate cancer. Oncogene 2018;37:710–21. [PubMed: 29059155]
51. Scher HI, et al. Increased survival with enzalutamide in prostate cancer after chemotherapy. N Engl J Med 2012;367:1187–97. [PubMed: 22894553]
52. James ND, et al. Abiraterone for Prostate Cancer Not Previously Treated with Hormone Therapy. N Engl J Med 2017;377:338–51. [PubMed: 28578639]
53. Kong Y, et al. Inhibition of cholesterol biosynthesis overcomes enzalutamide resistance in castration-resistant prostate cancer (CRPC). J Biol Chem 2018;293:14328–41. [PubMed: 30089652]
54. Mostaghel EA, et al. Resistance to CYP17A1 Inhibition with Abiraterone in Castration-Resistant Prostate Cancer: Induction of Steroidogenesis and Androgen Receptor Splice Variants. Clin Cancer Res 2011;17:5913–25. [PubMed: 21807635]
55. Taplin ME, et al. Androgen receptor mutations in androgen-independent prostate cancer: Cancer and Leukemia Group B Study 9663. J Clin Oncol 2003;21:2673–8. [PubMed: 12860943]
56. Volmer R, Ron D. Lipid-dependent regulation of the unfolded protein response. Curr Opin Cell Biol 2015;33:67–73. [PubMed: 25543896]
57. Corazzari M, Gagliardi M, Fimia GM, Piacentini M. Endoplasmic Reticulum Stress, Unfolded Protein Response, and Cancer Cell Fate. Front Oncol 2017;7:78. [PubMed: 28491820]
58. Lee AH, Scapa EF, Cohen DE, Glimcher LH. Regulation of hepatic lipogenesis by the transcription factor XBP1. Science 2008;320:1492–6. [PubMed: 18556558]
59. Richards K, Liou JI, Cryns V, Downs T, Abel J, Jarrard D. Metformin Use Is Associated with Improved Survival in Veterans with Advanced Prostate Cancer on Androgen Deprivation Therapy. J Urol 2017;197:E715–E716.
60. Nieland TJ, et al. Identification of the molecular target of small molecule inhibitors of HDL receptor SR-BI activity. Biochemistry 2008;47:460–72. [PubMed: 18067275]

SIGNIFICANCE

Findings highlight SR-B1 as a potential target in primary and castration-resistant prostate cancer that is essential for cholesterol uptake needed to drive steroidogenic and non-steroidogenic biogenic pathways.

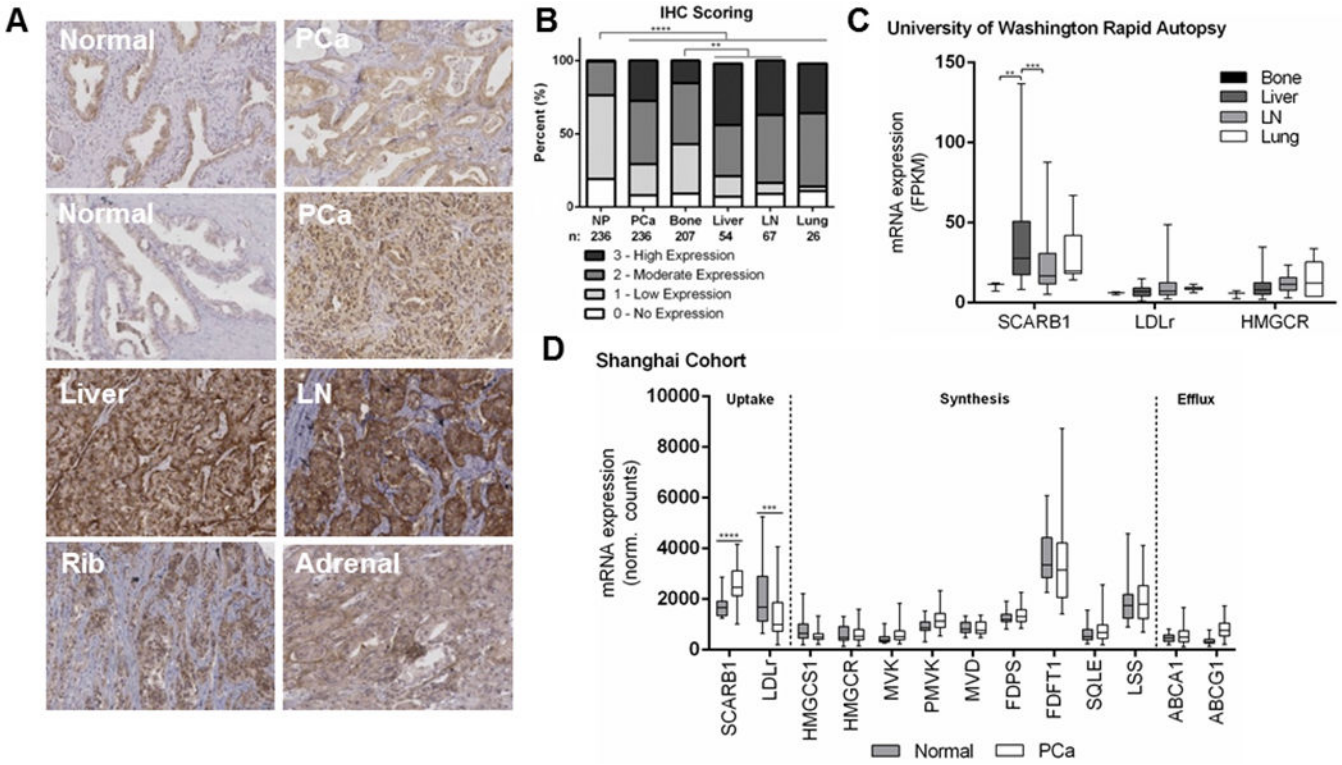

Figure 1: SR-B1 expression is increased in prostate cancer and persists in metastatic lesions.

(A) SR-B1 expression assessed by IHC in samples from the UWRA program and **(B)** scored by independent pathologists. (Normal/NP = Normal prostatic tissues, PCa = primary prostate cancer, Liver = Liver metastasis, LN = Lymph node metastasis, Rib = Rib bone metastasis, Adrenal = Adrenal metastasis). The mRNA expression was assessed from available expression datasets. **(C)** The expression of SR-B1 (SCARB1), LDLr and HMGCR by site of metastasis from the UWRA database (n = 83) presented as fragments per kilobase million (FPKM, middle line: median, box: 25th to 75th percentile, bars: min. to max.) **(D)** Normalized mRNA sequencing counts of SCARB1 and other cholesterol metabolism genes were analyzed from the Shanghai Cohort dataset. Expression levels are presented as normalized reads (middle line: median, box: 25th to 75th percentile, bars: min. to max.) and assessed in PCa (n = 28) as compared to matched normal prostatic tissue (Normal, n = 27). **p < 0.01, ***p < 0.001 ****p < 0.0001 by chi-square test **(B)** and ANOVA with Sidak's Test **(C,D)**.

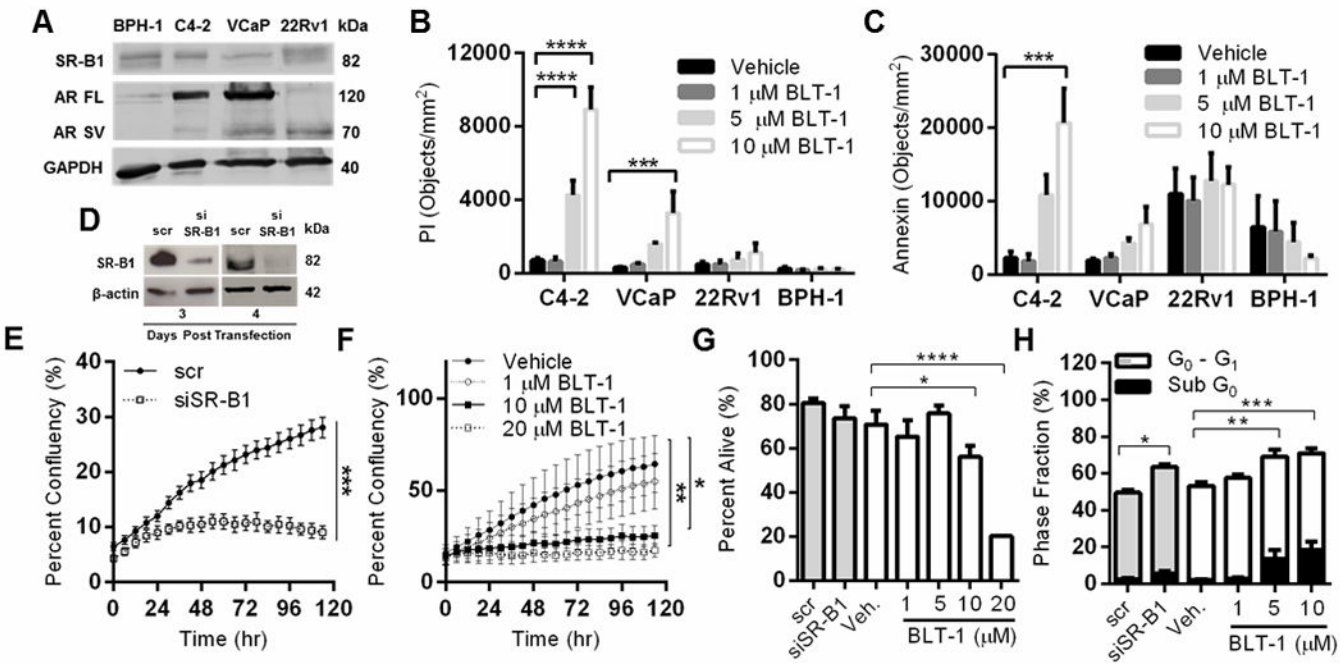

Figure 2: SR-B1 antagonism inhibits cell growth and induces cell cycle arrest in AR-driven PCa cells.

(A) SR-B1 and AR full length (FL) and splice variant (V7) expression were compared in BPH-1, C4-2, VCaP and 22Rv1 cells normalized to GAPDH levels by immunoblotting. The effect of SR-B1 antagonism on viability of this set of cells treated with vehicle and BLT-1 at 1, 5 and 10 μM was assessed by automated imaging growth analysis by **(B)** propidium iodide, and **(C)** annexin V staining (n = 3). **(D)** Expression of SR-B1 in C4-2 cells following either scramble (scr-) or SR-B1 targeted siRNA (siSR-B1) transfection normalized to β-actin levels by immunoblotting. Cellular growth assays were conducted for **(E)** scr- and siSR-B1-C4-2 cells, and **(F)** C4-2 cells treated with vehicle and 1, 10 and 20 μM BLT-1, with confluency measurements taken every 6 h (n = 3). **(G)** Live/dead assay of scr- vs. siSR-B1-C4-2 and vehicle vs BLT-1-treated cells assessed by the ratio of calcien AM-positive to ethidium homodimer-positive cells by flow cytometry (n = 3). **(H)** Cell cycle analysis of scr- vs siSR-B1-C4-2 and vehicle vs BLT-1-treated cells by propidium iodide staining and flow cytometry. Graphed is the percent of cells in G_0-G_1 phase (white/grey) and cells with sub G_0 DNA content (black) (n = 3). Data represent the mean ± SEM. *p < 0.05, **p < 0.01, ***p < 0.001 ****p < 0.0001 by ANOVA with Tukey's Test **(B, C, G, and H)** or by linear regression as discussed in results **(E and F)**.

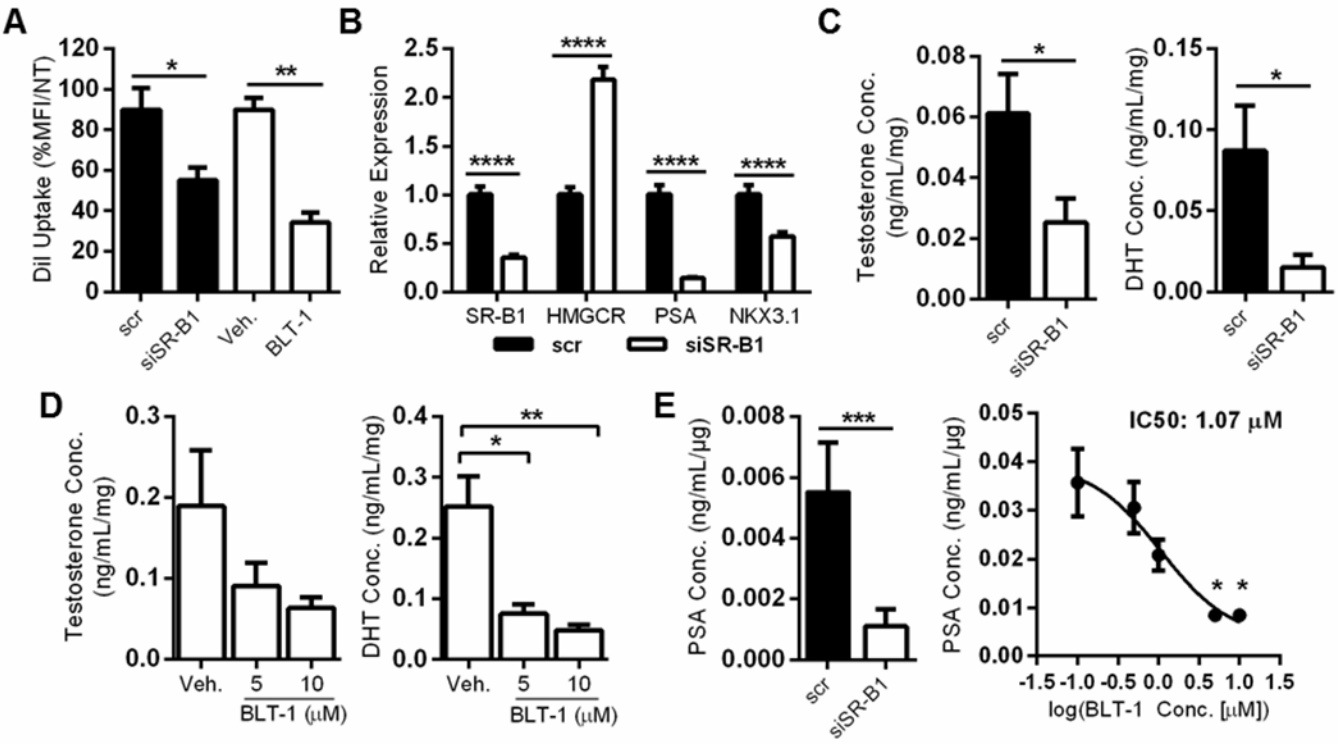

Figure 3: SR-B1 antagonism alters cholesterol metabolism, and reduces cellular androgen accumulation and AR activity, in C4-2 cells.

(A) Cholesterol uptake assessed by DiI-HDL and flow cytometry in C4-2 cells after either SR-B1 siRNA (siSR-B1) silencing or BLT-1 treatment as compared to scramble (scr)- and DMSO (Veh.)-treated cells, respectively (n = 3). Mean fluorescent intensity was normalized to the mean fluorescent intensity of non-treated cells incubated with DiI-HDL. **(B)** Expression of cholesterol metabolism (SCARB1 and HMGCR) and AR-regulated (PSA and NKX3.1) gene transcripts was assessed in siSR-B1- vs scr-C4-2 cells by qPCR (n = 3). Inserted are SR-B1 (upper) and β-actin (lower) immunoblots of the same lysates. Testosterone and DHT levels were measured by LC-MS to assess alterations in androgen accumulation in in siSR-B1- vs scr-transfected **(C)**, or in Veh.- vs 5 and 10 μM BLT-1 **(D)** treated C4-2 cells (n = 3). **(E)** PSA secretion into media was assessed by Cobas immunoassay (ng/mL) and normalized to cell density by plate protein content (μg) comparing scr- to siSR-B1-C4-2 cells (left), and BLT-1 from 0.1 to 10 μM (right). The later was also used to calculate an IC_{50} (n = 3). Data represent the mean ± SEM. *p < 0.05, **p < 0.01, ***p < 0.001 ****p < 0.0001 by ANOVA with Sidak's Test **(A, B)**, Student's T-Test **(C,E)**, ANOVA with Tukey's Test **(D,E)**.

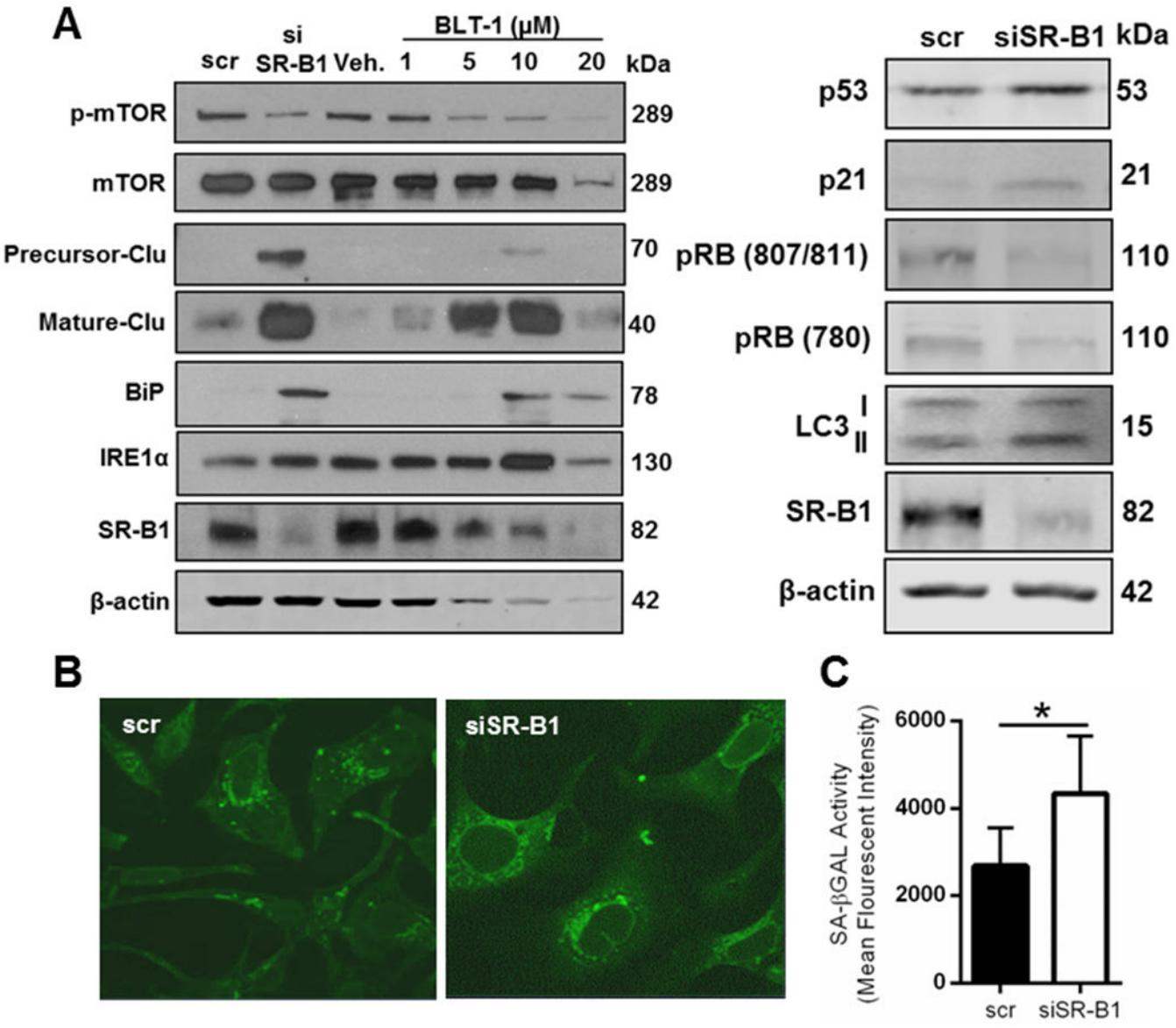

Figure 4: SR-B1 antagonism induces cell stress and activates autophagy pathways.

(A) Representative western blot analysis of autophagy and ER stress pathway markers in scr- and siSR-B1-C4-2 cells, or vehicle (Veh.) and BLT-1-treated C4-2 cells (n = 3). **(B)** Membrane staining of intracellular vacuoles and ER/Golgi blebbing in scr- and siSR-B1-C4-2 cells visualized by Alexa Flour-conjugated wheat germ agglutinin to image intracellular membrane structures by confocal microscopy. **(C)** SA-βgal activity in chloroquine treated scr- and siSR-B1-C4-2 cells assessed by C_{12}FDG and flow cytometry analysis (n = 7). Data represent the mean ± SEM. *p < 0.05 by Student's T-Test **(C)**.

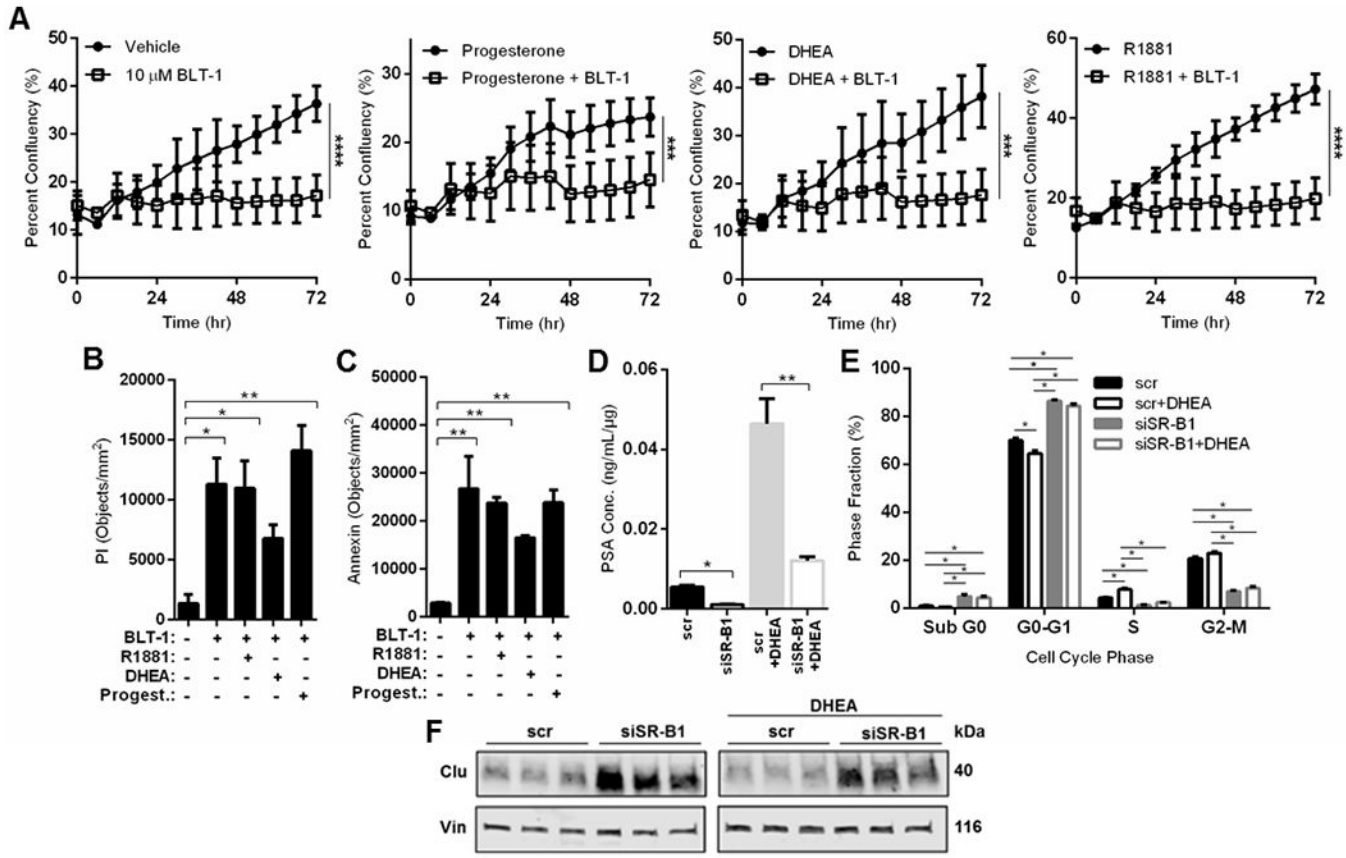

Figure 5: Arrested SR-B1 antagonized phenotype is not rescued by exogenous steroid.

C4-2 cells were incubated in the presence of BLT-1 (10 μM) alone (left), and progesterone (10 mM), DHEA (2.5 μM), or R1881 (10 nM) and assessed for cell growth **(A)** and cell death by propidium iodide **(B)** and annexin **(C)** staining (n = 3). scr- and siSR-B1 C4-2 cells cultured ±DHEA (2.5 μM) were assessed for the impact on **(D)** PSA secretion into media (n = 3), **(E)** the proportion of cells in different cell cycle phases as determined by propidium iodide staining and flow cytometry (n = 3) and **(F)** Clu expression normalized to vinculin (Vin) by immunoblotting (n = 3). Data represent the mean ± SEM. *p < 0.05, **p < 0.01, ****p < 0.0001 by ANOVA with Tukey's Test.

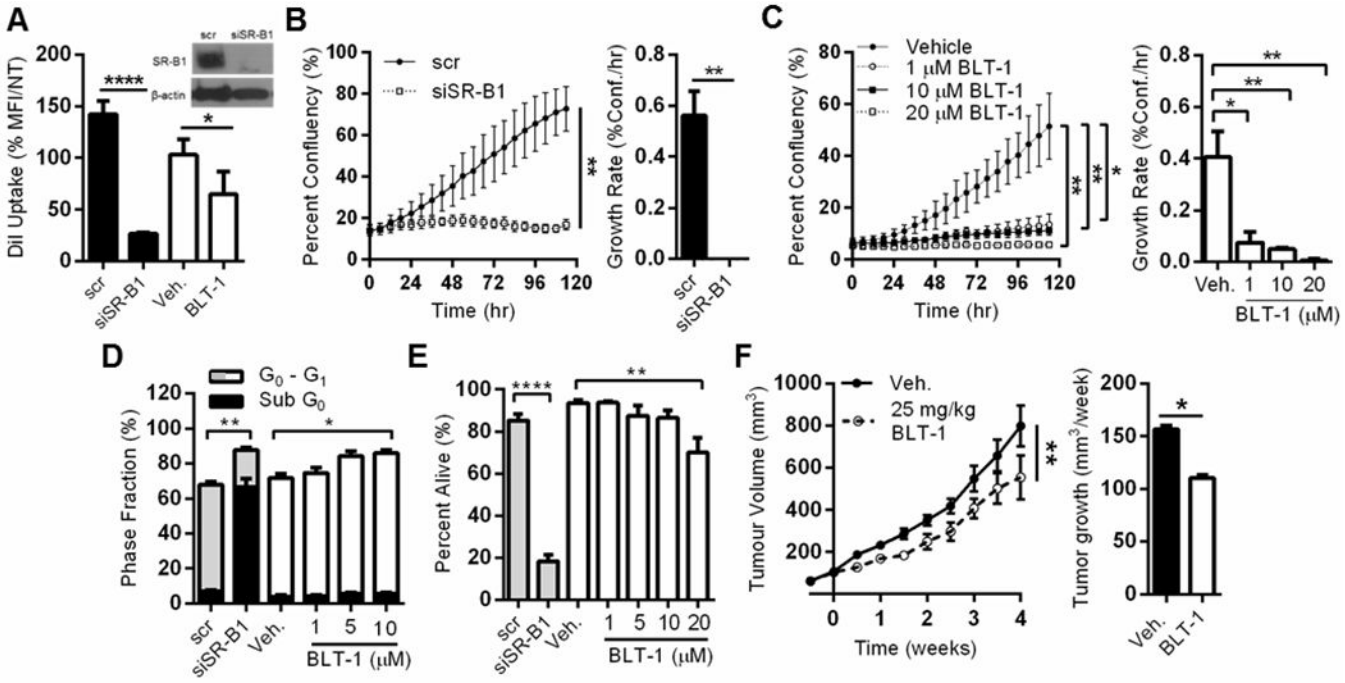

Figure 6: SR-B1 antagonism reduces cholesterol uptake and induces cell and tumor growth arrest in PC3 CRPC cells.

(A) siSR-B1-PC3 cells and PC3 cells treated with 10 μM BLT-1 assessed for uptake of DiI compared to scr-SR-B1-PC3 cells or vehicle treated cells (n = 3). Mean fluorescent intensity was normalized to the mean fluorescent intensity of non-treated cells incubated with DiI-HDL. Inserted are SR-B1 (upper) and β-actin (lower) immunoblots of the same lysates. **(B)** scr- and siSR-B1-PC3 cells, and **(C)** PC3 cells treated with vehicle and 1, 10 and 20 μM BLT-1, with confluency measurements taken every 6 h (n = 3). **(D)** Live/dead assay of siSR-B1-PC3 and PC3 cells treated with BLT-1 from 1 to 20 μM for ratio of ethidium homodimer and calcein AM staining to calculate the percentage of live cells as compared to scr-PC3 and vehicle-treated PC3 cells, respectively (n = 3). **(E)** Cell cycle analysis of siSR-B1-PC3 and BLT-1 treated cells by propidium iodide staining and flow cytometry plotted to show the fraction of cells in G_0-G_1 phase (n = 5). **(F)** PC3 xenograft bearing mice were treated with BLT-1 (25 mg/kg) once daily by oral gavage and monitored for tumor growth over time vs vehicle dosed animals (n = 12). Data represent the mean ± SEM. *p < 0.05, **p < 0.01, ****p < 0.0001 by ANOVA with Sidak's Test **(A)** or Tukey's Test **(D, E)** and linear regression as discussed in results **(B,C,F)**.